

# Biomechanical Energy Harvesting System With Optimal Cost-of-Harvesting Tracking Algorithm

Alon Cervera, *Student Member, IEEE*, Ze'ev Rubinshtein, Moran Gad, Raziel Riemer, and Mor Mordechai Peretz, *Member, IEEE*

**Abstract**—Biomechanical energy harvesting can provide an attractive alternative for powering portable electronics, such as laptops and mobile communication devices. This unique type of energy is particularly advantageous to those who do not have direct access to the utility grid for extended periods of time. This paper presents an innovative biomechanical energy harvesting system based on the regenerative braking concept applied to the human natural motion. To determine the optimal braking profile, previous studies used an offline procedure based on constant external load to determine the optimal braking profile. The new concept of this paper continuously optimizes the maximum amount of energy that can be extracted during human motion while minimizing the subject's effort (metabolic rate). This is achieved by an energy harvesting system equipped with a programmable braking profile and a unique power extraction algorithm, which adaptively changes the braking profile to obtain the optimal ratio of energy to effort. These are facilitated by a brushless dc generator that is connected to boost converter. A digital current-programmed control of the boost converter enables an adaptive torque variation according to biofeedback (the measure of effort) and electrical feedback. This paper focuses on the human knee joint as the energy source, since most of this joint's work during level walking is negative (muscles are acting as brakes). Since this paper is preliminary and more oriented to the novel concept of adaptive profile and optimal power extraction, the operation of the energy harvester is demonstrated on a full-scale laboratory prototype based on a walking emulator. Initial experiments on human subjects have been initiated and are also reported. The results exhibit ultimate power extraction capabilities as well as adaptation to the walking pattern.

**Index Terms**—Biomechanics, energy harvesting, optimal control.

## I. INTRODUCTION

WITH the increasing use of portable electronics, there is a growing demand for portable, preferably renewable, sources of power. An emerging technology is biomechanical energy harvesting [1]–[8]. This technology uses

Manuscript received February 22, 2015; revised August 7, 2015 and October 23, 2015; accepted December 20, 2015. Date of publication January 1, 2016; date of current version January 29, 2016. Recommended for publication by Associate Editor M. Molinas.

A. Cervera, Z. Rubinshtein, and M. M. Peretz, are with the Center for Power Electronics and Mixed-Signal IC, Department of Electrical and Computer Engineering, Ben-Gurion University of the Negev, Beersheba 8410501, Israel (e-mail: cervera@bgu.ac.il; zeev.rubinshtein@gmail.com; morp@ee.bgu.ac.il).

M. Gad is with the Department of Mechanical Engineering, Ben-Gurion University of the Negev, Beersheba 8410501, Israel (e-mail: morangad@gmail.com).

R. Riemer is with the Department of Industrial Engineering and Management, Ben-Gurion University of the Negev, Beersheba 8410501, Israel (e-mail: rriemer@bgu.ac.il).

Color versions of one or more of the figures in this paper are available online at <http://ieeexplore.ieee.org>.

Digital Object Identifier 10.1109/JESTPE.2015.2514079

TABLE I

TYPICAL ACTIVITY OF DIFFERENT JOINTS PER SINGLE STEP

Joint	Work [J]	Power [W]	Max. Torque [Nm]	Negative Power [%]	Negative Power [W]
Heel strike	1-5	2-10		50	1-5
Ankle	33.4	66.8	140	28.3	19
Knee	18.2	36.4	40	92	33.5
Hip	18.96	38	40-80	19	7.2
Elbow	1.07	2.1	1-2	37	0.8
Shoulder	1.1	2.2	1-2	61	1.3

human natural motion, e.g., walking, to generate energy. The motivation of this approach stems from the fact that the average energy density of food is 35–100 times higher than batteries. Moreover, during a day of activity, a person uses  $\sim 10.7$  MJ [3] of energy. To store this amount of energy using batteries, a bank of  $\sim 20$  kg is required. Harvesting small amounts of this energy, without affecting the motion, can power or recharge portable devices. As a consequence, the weight of batteries may be reduced, and extended operational time between utility grid charges is achieved. Potential usage of such technology is aimed for travelers and hikers, who cover extended distances with limited supply, assistance in disaster areas, and military.

During a single step of a human subject, the muscles perform both positive work to generate forward motion and negative work to absorb residual kinetic energy and control the motion [9]–[11]. Similar to the concept of regenerative braking in electric vehicles [1], to perform the required negative work, the kinetic energy can be converted into usable energy using an electric generator. Otherwise, the energy is dissipated entirely as heat within the body by pure muscle effort [12]. In this context, the knee joint stands out of all the other body joints (Table I) with the highest negative work of 33.5 J per step for both knees for 80-kg subject walking on a plane surface at a normal speed ( $\sim 1$  Hz) [3].

The common terminology to quantify the efficiency of harvesting is by the cost of harvesting (COH) [1], which is defined as the ratio between the difference in the metabolic energy of walking with the device when harvesting and when disengaged mechanically ( $\Delta$  metabolic energy) and the difference of extracted electrical energy with and without harvesting ( $\Delta$  electrical energy)

$$\text{COH} = \frac{\Delta \text{metabolic energy}}{\Delta \text{electrical energy}}. \quad (1)$$

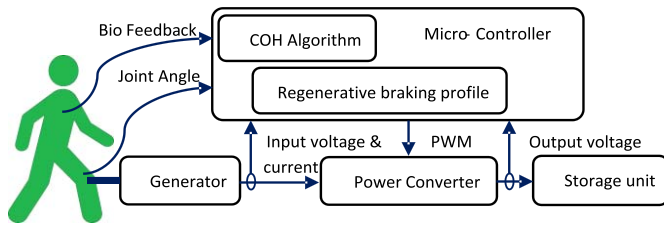


Fig. 1. Block diagram description of the interaction between a human subject and the electromechanical harvester. The harvester is managed by a microcontroller unit which receives control information from both the human and the harvester.

The goal of efficient harvesting is to reduce the COH as much as possible, i.e., to increase the metabolic efficiency of the human walking. This is done by optimizing the portion of harvested electrical energy from negative muscle work. Naturally, if the extracted energy exceeds the amount of negative work available, the motion is disrupted, and the subject has to perform extra (positive) work to maintain balance. Therefore, at all conditions, the braking torque applied to the joint must be smaller than the joint muscle natural torque (i.e., torque performed by the knee during walking with no device). Furthermore, matching the braking torque to the natural joint torque does not yield the best results [3]. In this case, all the human motion is controlled by the device, while the muscles are not active, which is not feasible for able-bodied humans (i.e., without disability). The subject of applied torque profile that yields the best COH results is still an open subject in the biomechanical community and is beyond the scope of this paper.

Previous studies on biomechanical harvesters have reported power output range of up to  $\sim 8$  W [1], [3]–[8], [13]–[19]. Therefore, systems were designed to achieve maximum energy at a given level of effort. A true regenerative system that extracts and stores the energy as well as optimizes the COH has not been reported hitherto.

The objective of this paper is to introduce a biomechanical energy harvesting system that minimizes the walking effort (COH) of a human subject by applying a regenerative braking operation without interference to the subject's motion. As a result of the regenerative braking action, usable electrical energy is gained that can further save on weight to be carried. This is achieved by a minimization algorithm that controls the harvesting system and adjusts the torques profile to achieve the lowest COH at a given set of conditions. This is required since the optimal braking torque that will produce the lowest COH varies from one subject to another, type of surface, motion pace, and more [20]. The preliminary work, originally presented in [21], has been expanded in this paper by in-depth theoretical analysis and initial experiments on human subjects by a custom-made knee brace setup.

The closed-loop harvesting system is conceptually shown in Fig. 1. It consists of a generator to convert motion into electricity, a boost converter that operates in a current-programmed mode to achieve the desired torque pattern, while extracting energy, and a storage unit (battery plus charger). An additional feedback loop is added to track the optimal COH point.

The performance of the tracking system, to-date, is examined using a walking emulator, and the information of the COH is synthesized into the system. It should be noted that all experiments on human subjects were approved by the Ben-Gurion University of the Negev Human Research Institutional Review Board and were carried out on a monitored treadmill, having all participants' written consent. The results of energy harvesting with human subjects are currently demonstrated, as prescribed by the commission, without active (closed loop) tracking procedure.

## II. KNEE JOINT AS A POWER SOURCE

In human walking, the knee joint performs a periodic motion where a single step is defined as a period. Fig. 2 shows a typical knee-joint activity during a period, for the values of [Fig. 2 (top to bottom)]: 1) angle (zero represents a straight leg position); 2) velocity; 3) torque; and 4) power [3]. The period is separated into four sections according to flexion and extension of the knee (J1–J4). As can be observed from Fig. 2, by calculating the instantaneous product of the applied torque on the joint and the velocity, the areas of negative work can be identified, and these are marked as K1, K3, and K4. As a result, the knee joint can be considered as a low-frequency pulsating power source with relatively low angular speed ( $< 5$  rad/s).

Direct measurement of the knee-joint torque is not feasible, and methods for estimating the knee net muscle torque require equipment that is complex and hard to fit on the knee. Therefore, an alternative approach based on the information of the joint angle and the rotation velocity is taken to identify the regions J1–J4. The joint rotation velocity can be extracted by taking the derivative of the angle. In this way, only one sensor of the joint angle is required. This approach is based on the observation that each section of negative work ends at zero velocity and different joint angles for each section [20]. Using this information, an algorithm that identifies the particular portion of the step has been developed.

An algorithm for identification of J1–J4 is realized by detecting the zero crossing instance of the velocity curve (e.g., transition from negative slope to a positive one), and capturing the angle value at this instance. The maximum angle value of all zero crossing points would correspond to the beginning of section J4. Since the angle value of J4 is significantly higher than in the other sections, the identification of J4 is simplified and is obtained by comparison against the angle median value rather than a maximum search. Once J4 is identified, the other sections are easily obtained by the zero crossing detection, given a periodic walking pattern.

Since the walking profile may vary, a refinement of the detection procedure is facilitated by an adaptive algorithm in which the system is learning the walking profile of the subject. This adaptive process is explained in more detail by the flowchart of Fig. 3. At system boot, a straight leg and a starting point at J1 section are assumed as well as an initial joint angle median. In the first periods (several walking steps), the system does not perform harvesting and is dedicated for learning the walking pattern of the subject. The process of

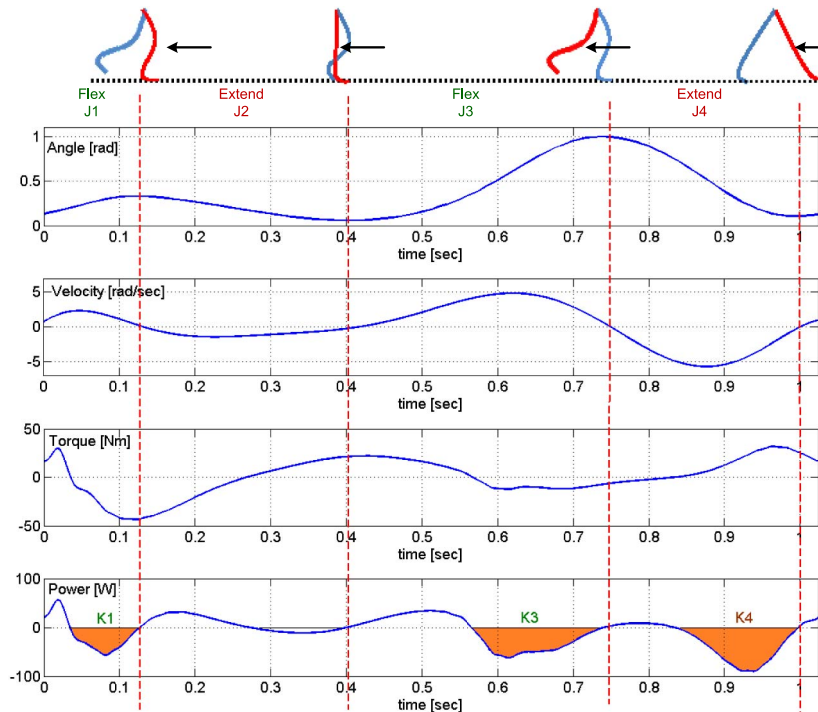


Fig. 2. Physical parameters for a knee joint for one rotation cycle. Top to bottom: angle, velocity, torque, and power. The knee movement can be divided into four characteristic segments J1–J4, portrayed on top. Areas with negative work are marked as K1, K3, and K4.

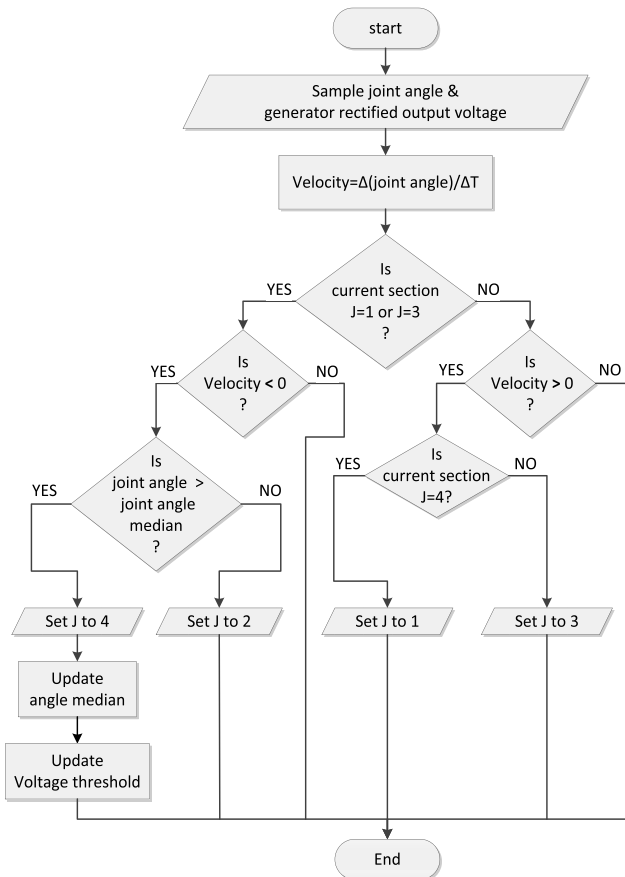


Fig. 3. Adaptive algorithm to obtain the knee-joint position through time.

joint angle median refinement is iterative and is updated every period. It can also be seen from Fig. 2 that only a portion of the sections J1, J3, and J4 have negative work. Therefore, to avoid

inducing torque on the subject at false location, once a region that contains negative work is detected (e.g., J4), the system monitors the rectified generator voltage (which is proportional to the rotation speed in a synchronous brushless machine) and triggers the harvesting command when it has reached a programmable threshold, relative to the maximum voltage. This ratio has been selected from experimental joint data mining by a trial and error procedure which has been found suitable to accommodate the power stage practical limits while maintaining smooth walking pattern. The angle median and the voltage threshold values are updated every period with the detection of J4.

### III. HARVESTING SYSTEM

The electromechanical system used in this paper consists of a walking emulator (that will be replaced by a knee brace for experiments on human subjects’), configured to emulate knee motion and assembled, such that the knee motion drives a gear train through a unidirectional clutch, transmitting only knee flexion motion to a brushless dc (BLdc) generator [22]. A simplified block diagram of the electrical harvesting system is shown in Fig. 4.

The three-phase BLdc generator is followed by a rectifier. The rectifier is constructed by a three-phase bridge topology that can facilitate either passive or synchronous rectification. The passive mode comprises a classic three-phase diode bridge. The main advantage of this rectification type is its simplicity, i.e., it does not require active control or sensors for operation.

Synchronous mode rectification utilizes a three-phase transistor bridge configuration. Therefore, the transistors are commutated according to the states of Hall effect sensors,

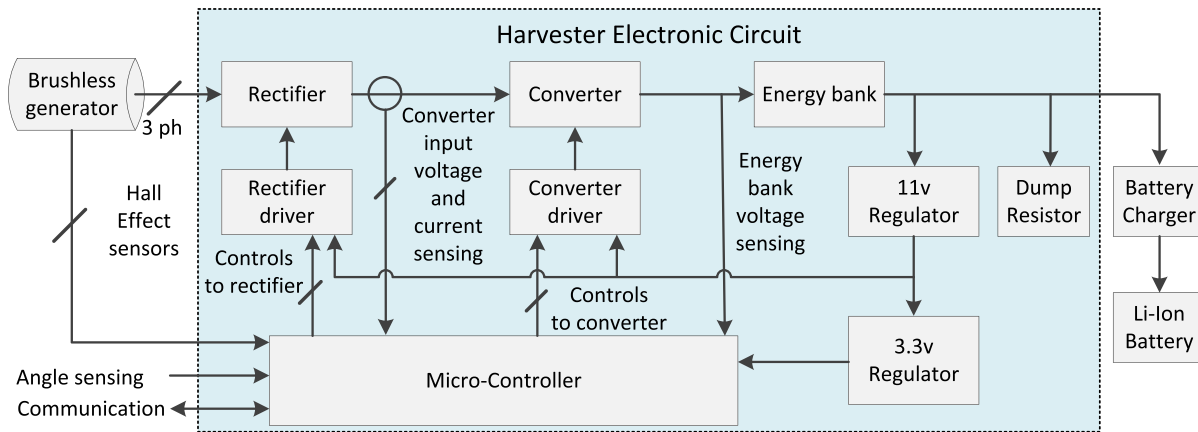


Fig. 4. Block diagram of the hardware for the energy harvester.

embedded in the BLdc generator. The latter is generally preferred if the generator is rated for low voltages, where the diodes' voltage drop becomes a dominant loss contributor. To reduce the losses during synchronous rectification, the Hall effect sensors are powered only during active harvesting periods.

To enforce a desired braking profile on the BLdc generator, an average current-controlled boost converter is employed. This is enabled by the linear relationship between the BLdc generator current and the induced resistive torque [22], [23]. A current sourcing behavior is vital, since the generator output voltage and the required resistive torque are not directly linked, as shown in Fig. 2. The boost converter output is linked to a capacitive energy bank to filter the low-frequency discontinuous current caused by the human walking profile, and to provide dc voltage with acceptable ripple for the power consumer. To demonstrate the practical utilization of the harvested energy, an off-shelf Li-ion battery charger is used as a generic load.

In the context of this paper, it is important to demonstrate the capabilities of the harvesting system to extract all the available power from negative work (within the limits that prevent convenient walking profile as described earlier), regardless of the load state or the instantaneous consumption of device specific load. Since a specific load-oriented voltage control loop has not been realized, and to prevent overvoltage when unloaded, a dumping resistor with autonomous control is used. By doing so, any generic load (battery charger in this case) can be connected without any need to change or redesign the system. Furthermore, the system is self-contained as the output, linked by the boost's diode to the generator, serves as the power source for the controller and peripherals.

The power harvesting system is digitally controlled. The system operation concept is described by the flowchart in Fig. 5. The controller operates in one of two modes: 1) wake-up and 2) free-run. In the wake-up mode, the system does not actively harvest energy, and the BLdc generator voltage breaches the rectifier diodes and charges the output energy bank with minimal amount of energy. This energy is used to power up the microcontroller. In the first three walking

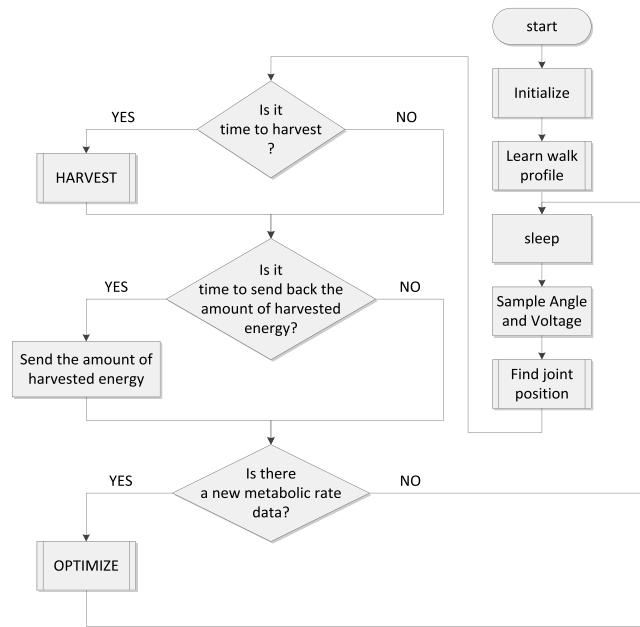


Fig. 5. Average current mode boost with generic braking profile.

steps, the microcontroller works in low-power mode while learning the subject walking profile.

The free-run stage has two modes of operation: 1) harvesting; and 2) no-harvesting. The no-harvesting mode is similar to wake-up phase, the power stage is set in sleep mode, and the microcontroller is programmed to wake up every 8.25 ms and sample the knee-joint angle to keep track on the key parameters (angles, speed, and knee position in step period) while looking for the areas of negative work. The difference between the wake-up phase and the no-harvesting mode is the communication with external systems (e.g., metabolic cart), where the system periodically monitors the data on the amount of harvested energy and checks if new user metabolic rate data are available.

Once a negative work area has been detected, the system shifts to harvest mode. Here, all system resources are activated, the generator's Hall effect sensors are turned ON, and the

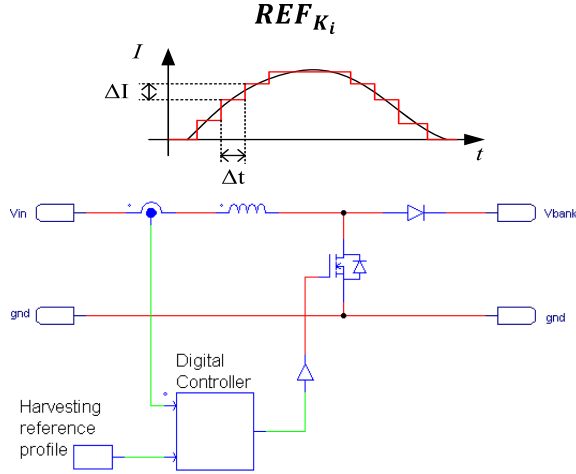


Fig. 6. Conceptual flowchart of the controller's main routine.

rectifier operation is set for synchronous switching. Average current-programmed mode operation forces the boost average inductor current to follow a specified braking profile ( $REF_{K_i}$ ) that is constructed, in this paper, from two arrays named base ( $BASE_{K_i}$ ) and delta ( $DELTA_{K_i}$ ), for each negative working area ( $K_i$ ) (Fig. 6).

The base array contains an initial generic current profile that allows energy to be harvested from a subject without affecting user's natural motion. This array is loaded to the reference profile during system boot

$$REF_{K_i}(n) = BASE_{K_i}(n) \quad (2)$$

where  $n$  is the array cell index and  $i$  is the index of the  $K_i$ th section.

To allow online adjustment of the braking profile, i.e., shaping the current pattern, the current reference to the boost controller ( $REF_{K_i}$ ) is constructed by the summation of the reference and the delta arrays and can be expressed as

$$REF_{K_i}(n) = REF_{K_i}(n) \pm DELTA_{K_i}(n). \quad (3)$$

As opposed to the base array which is fixed, the delta array can be updated on-the-fly. As a result, a flexible current reference of any shape and magnitude may be applied on the subject for evaluation and further optimization of the harvesting. It should be noted, however, that to-date, the issue of the optimal harvesting profile is still an open issue in the biomechanical community. Therefore, the emphasis in this paper has been on shifting the generic base profile, rather than realizing various braking profiles.

Following the current profile, the harvested energy is transferred to an energy bank (capacitor  $C$ ). The sizing of  $C$  is obtained, such that when unloaded, an entire step of maximum harvested energy ( $E_{in_{max}}$ ) can be stored while remaining within a predefined voltage swing  $\{V_{min}, V_{max}\}$  by

$$C = 2E_{in_{max}} / (V_{max}^2 - V_{min}^2). \quad (4)$$

The designed boost converter has a practical voltage gain limitation of approximately 7–8; therefore, the upper voltage

bound of the energy bank sets the converter minimum operating voltage. Since the region detection procedure already monitors the generator voltage (for harvesting on negative work regions), the minimum operating voltage serves as the minimum threshold to trigger harvesting.

Since the information of the input voltage and the current is readily available and is required for the COH minimization routine, the controller calculates the amount of harvested energy over a single step as follows:

$$E_{in_{step}} = \sum_n V_{in}(n) I_{in}(n) \Delta T \quad (5)$$

where  $\Delta T$  is the time between samples, and  $V_{in}$  and  $I_{in}$  are the input voltage and the current to the boost converter, respectively.

#### IV. OPTIMAL COH TRACKING ALGORITHM

In theory, harvesting small amount of available negative energy should reduce the metabolic rate, in comparison with a case of carrying the harvesting device but not harvesting [12]. On the other hand, harvesting more than available negative energy would increase the metabolic rate. Furthermore, even in the case that exactly all the negative energy is harvested, then the metabolic rate would increase [3]. In such case, the device will perform all the joint control, and the human must not resist the forced action, i.e., not apply his knee muscles at all. Therefore, a reasonable conjecture is that there exists some level of support (harvesting during negative phase) that will be optimal. However, this optimal level has not been established yet by the biomedical community.

Following these arguments, a conjecture made in this paper is that a global minimum exists for the COH function of (1), and the object of the algorithm is to converge into this target point. The COH minimum location or value may vary from one harvesting profile to another, but it always exists. There might be a case that a braking pattern yields higher extracted energy than another (lower COH); however, this issue is still an open subject and is beyond the scope of this paper.

To facilitate easier realization of the COH tracking algorithm, and without losing generality, this paper expands the COH function of (1), so that ( $\Delta$  metabolic energy) and ( $\Delta$  electrical energy) relate between the difference of a present ( $j$ ) and previous ( $j-1$ ) obtained measurement (instead of active and inactive harvesters). Equation (1) can now be rewritten as

$$COH_j = \frac{(\text{metabolic energy})_j - (\text{metabolic energy})_{j-1}}{(\text{electrical energy})_j - (\text{electrical energy})_{j-1}}. \quad (6)$$

By doing so, the well-known maximum power point tracking algorithms can be adopted and implemented with readily available information. The algorithm that is selected to track the optimal COH is a modification of the hill-climbing concept [24]. Therefore, in case that the COH result is negative, the harvested energy is smaller than the optimal one, and the reference current profile is increased. On the other hand, when the COH is positive, the harvested energy is higher than the optimal amount and the reference is decreased (Fig. 7).

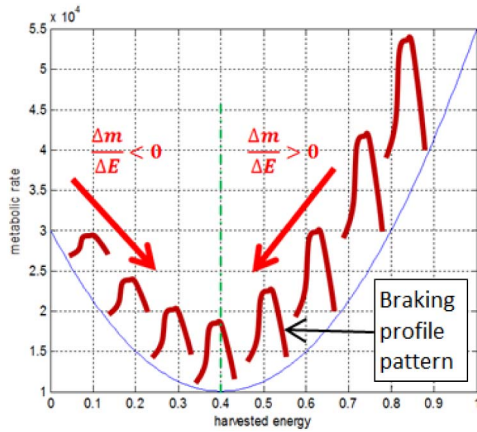


Fig. 7. Metabolic rate as a function of normalized harvested energy.

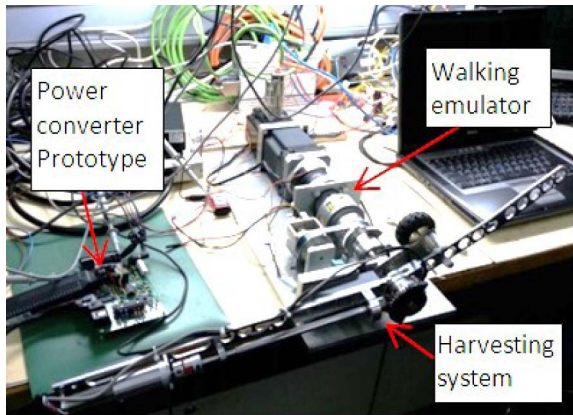


Fig. 8. Experimental setup with walking emulator and biomechanical energy harvesting system.

$REF_{K_i}$  (5) can then be adjusted according to

$$REF_{K_i,j} = REF_{K_i,j-1} - \text{sign}(\text{COH}_j) \times \text{DELTA}_{K_i}. \quad (7)$$

## V. EXPERIMENTAL RESULTS

To test the harvesting system and the optimal COH tracking algorithm in an isolated environment, a knee-movement emulator has been constructed. A photograph of the experimental setup is shown in Fig. 8. Fig. 9 shows a schematic block diagram of the system. The knee emulator has been custom constructed to integrate the exact specifications of the real knee brace and generator, and is driven using an off-shelf servo motor (Emerson Control Techniques). To increase the resolution and match the output torque of the human knee, a 10:1 gear train is added to the emulator motor before the mechanical hardware of the harvester. Knee-joint angles that correspond to human walking pattern were then programmed into the servo motor controller using a lookup table, factorized according to the gear train.

The experimental data of the emulator controller and the power stage have been viewed and recorded by the oscilloscope and the MATLAB. Since the device is not tested on human subjects, the metabolic rate data have been synthesized by the MATLAB script, where the metabolic energy curve was

TABLE II  
PARAMETERS OF BLdc GENERATOR [25]

Nominal voltage	18 V
No load speed	6710 rpm
No load current	294 mA
Nominal speed	5250 rpm
Nominal torque	96.9 mNm
Nominal current	3.54 A
Terminal resistance phase to phase	0.413 Ohm
Terminal inductance phase to phase	0.322 mH
Torque constant	25.1 mNm/A
Speed constant	380 rpm/V
Rotor inertia	135 gcm <sup>2</sup>

created as a parabola function of averaged electrical harvested energy ( $E_{in,av}$ ). The microcontroller transmits (through serial communication) to the PC the value of  $E_{in,av}$  and receives back the appropriate metabolic energy.

The key parameters of the BLdc generator used in the experimental setup (MAXON EC-45 flat) have been summarized in Table II [25]. Additional key components of the system were: 1) microcontroller: PIC24FJ32GA102 [26]; 2) auxiliary power supply: LTC3115-1; 3) energy bank: 12-mF capacitor (limited using a discharge resistor within the limits of 18–28 V); and 4) lithium-ion cell charger: LT3650-4.2. The off-shelf battery charger has been modified to draw the available amount of energy from the energy bank. This way the battery is charged continuously in semisteady state as the charging current fluctuates slightly according to energy bank voltage. Charging operation interrupted only when the energy bank voltage drops below the set minimum limit ( $V_{min}$ ). The boost input current measured with a resolution of 8 mA ( $\Delta I$ ), which gives the system a virtual mechanical resistance (i.e., braking) profile resolution of 16.6 mNm on the subject joint. The profile update is synchronized with the boost switching frequency (50 kHz) allowing a braking profile time step resolution as low as 20  $\mu$ s ( $\Delta T$ ).

Figs. 10 and 11 show the operation of the harvesting system by employing a constant torque (constant current) braking profile. The results show that the experimental system follows a given constant current reference profile, while harvesting from pulsating source. The energy bank voltage stays between the set limits, while the battery is charged continuously with current slightly fluctuating according to the energy bank voltage. Results of the optimal COH tracking algorithm as a function of algorithm iterations are shown in Fig. 12, which shows that the optimal COH point has been obtained within few iterations of the tracking algorithm. The system efficiency is shown in Fig. 13 as a function of the harvested power.

## VI. VERIFICATION ON HUMAN SUBJECTS

To further verify the operation of the biomechanical energy harvester and its compliance to human subjects, a full-scale laboratory setup has been constructed, as shown in Fig. 14. The setup consists of a customized knee brace, on which the BLdc generator and the gear train are mounted to (measured weight—1.5 kg), a computer-controlled treadmill

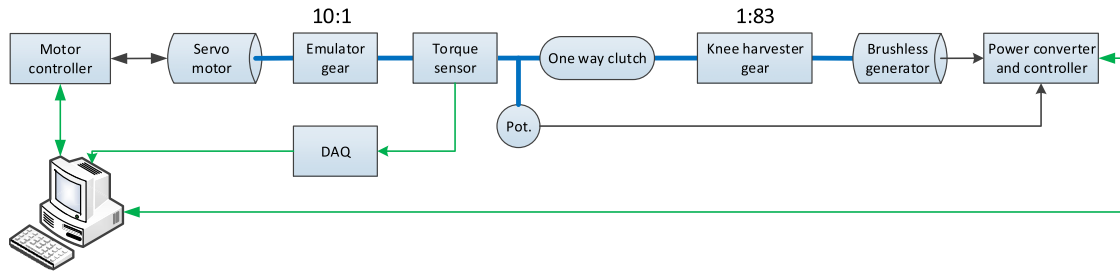


Fig. 9. Schematic block diagram of the experimental setup.

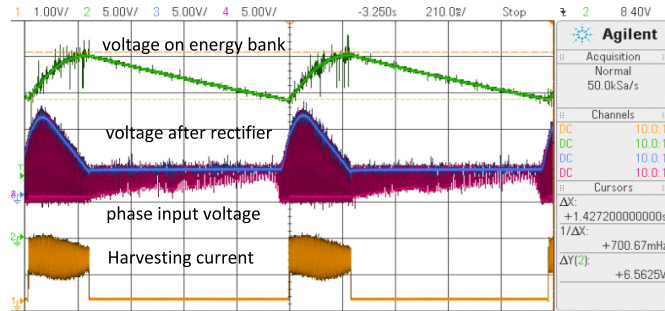


Fig. 10. Exemplary experimental results of the power harvester during regenerative braking action. The four channels measure (210 ms/div): boost input current (CH1, 1 V/div, 1 V/A), energy bank voltage (CH2, 5 V/div), boost input voltage (CH3, 5 V/div), and generator single-phase voltage (CH4, 5 V/div).

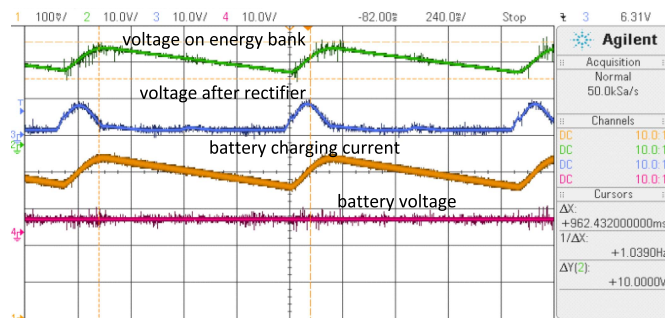


Fig. 11. Exemplary experimental results of the power harvester during regenerative braking action. The four channels measure (240 ms/div): battery charging current (CH1, 0.1 V/div, 4 V/A), energy bank voltage (CH2, 5 V/div), boost input voltage (CH3, 10 V/div), and battery voltage (CH4, 10 V/div).

(T2100 treadmill, General Electric Healthcare, USA), and an indirect calorimeter (Quark cpet, COSMED, Milano, Italy) to calculate the metabolic rate [27] for obtaining the COH. The harvester’s electronic hardware has been wired to the generator and located by the work bench to allow *in situ* measurements, while the experiment is conducted. The knee brace has been designed by a professional orthotist to enable free joint motion and comfortably remain in place for prolonged use.

The experiment measured harvesting in four intensity levels—0%, 15%, 30%, and 50% of the theoretical maximum negative work. For each measurement, a participant walked for 12 min with the treadmill set to a speed of 4.68 km/h with no gradient, then rested for at least 5 min. The 12 min were chosen to allow for the participant to reach stable aerobic levels

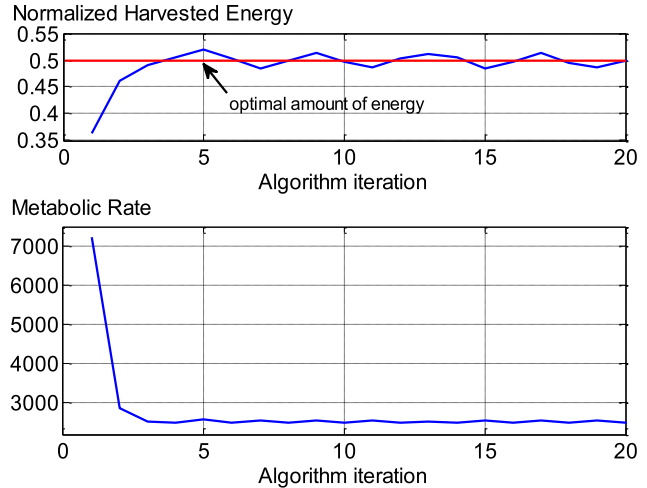


Fig. 12. Normalized harvested energy (top graph) and metabolic rate (bottom graph) as the functions of COH optimal algorithm iterations.

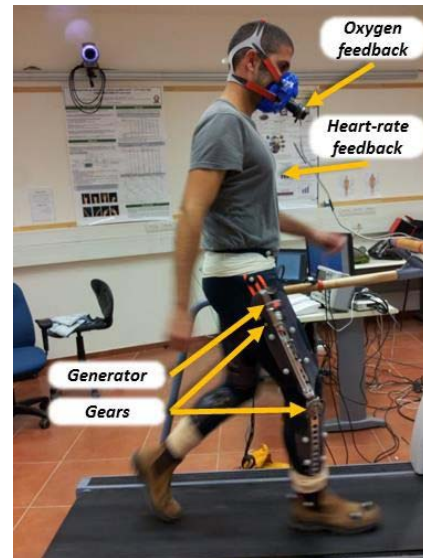


Fig. 13. Snapshot during experiment on a human subject, showing the laboratory setup.

and provide stable and consistent metabolic readings [1], [13]. The participants provided their full and informed consent by signing an informed consent form approved by the Ben-Gurion University of the Negev Human Research Institutional Review Board.

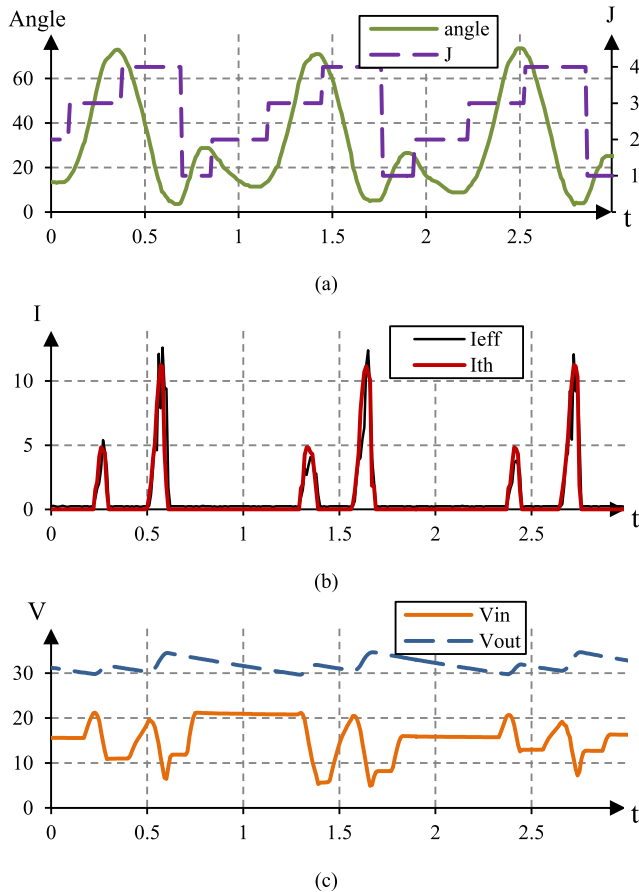


Fig. 14. Experimental waveforms from a human subject walking on the treadmill. (a) Angle and identified  $J$  region. (b) Harvest current (defined versus measured). (c) Input and output voltages of the power stage.

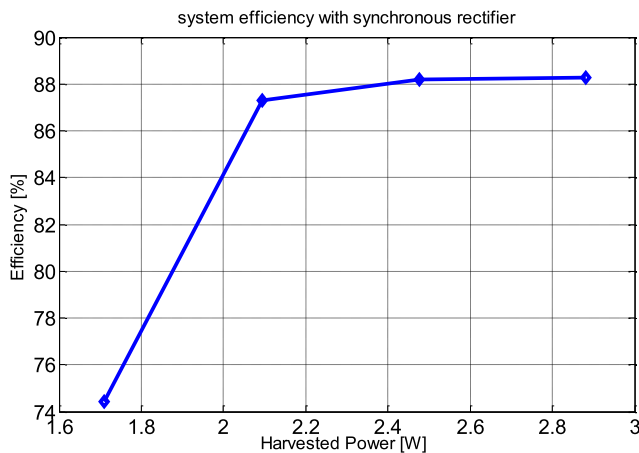


Fig. 15. System efficiency (does not include mechanical system and battery charger efficiencies) as a function of extracted power.

Fig. 15 shows the experimental waveforms of the walking pattern. The measured knee angle is in good agreement with the theoretical waveforms from Fig. 2, and the relevant regions (J1–J4) are correctly identified. In addition, the given and measured harvesting current profiles are presented, which demonstrate the capability of the power stage to produce the demanded torque for the experiment. Power consumption can

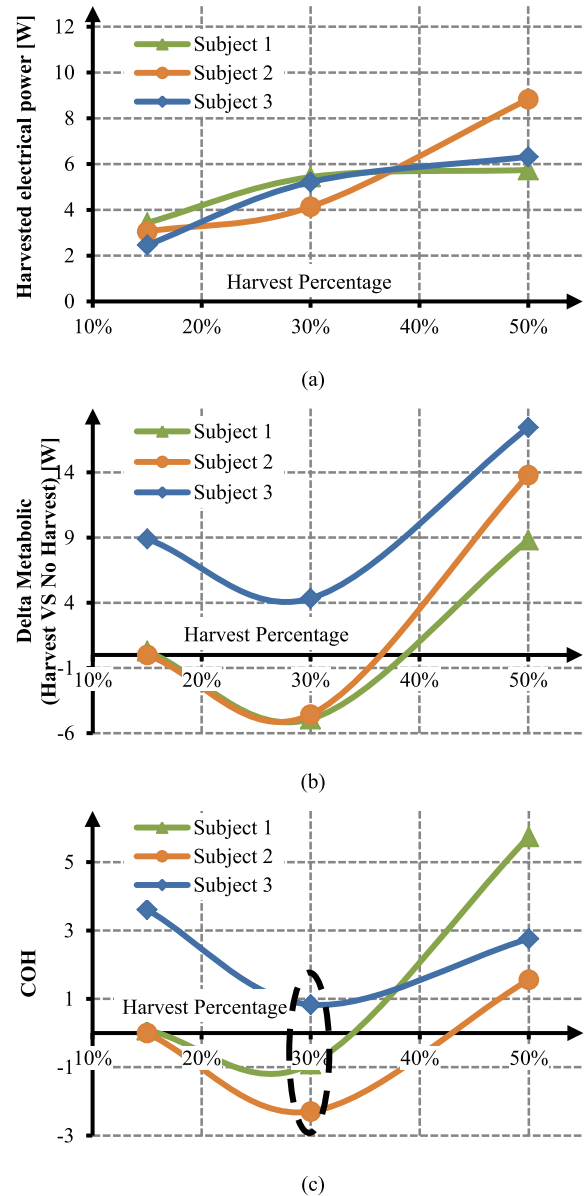


Fig. 16. Results of initial experiments on human subjects as a function of percentage of harvested power out of theoretical harvestable power. (a) Power generated from both legs. (b) Change in metabolic rate in relation to 0% harvesting. (c) COH with the minimum marked  $\sim 30\%$ .

be observed on the storage capacitor, from external loading, used to measure the produced power.

Further results of initial experiments for several subjects are shown next. Fig. 16(a) reveals consistent increase in output power as the harvesting profile is increased. Fig. 16(b) reveals a measurable decrease in metabolic rate when harvesting at 30% leading to a negative COH [Fig. 16(c)] for two subjects and a clear minimum for all three. The noted offset in the COH results from Subject 3 originates from mismatch between the experimental knee brace and the subject’s leg. The results of the initial experiments have reconfirmed the operation of the harvester for profile learning and variable torque profile. COH optimization experiments have yet to be conducted on human subjects. It is noted that the effect of the added weight

from the knee brace is not of consideration in this setup, since the results are in relation to walking with the brace without harvesting. The full set of results on these experiments is beyond the scope of this paper and will be the subject of further research.

## VII. CONCLUSION AND DISCUSSION

An energy harvesting system with optimal energy harvesting tracking algorithm has been presented. The experiments showed that the power harvester features adequate dynamic response with zero steady-state error. The optimal COH tracking algorithm has been demonstrated to successfully detect the negative work areas and harvest the optimal amount of energy.

The concept of regenerative braking, commonly used in electric or hybrid vehicles, has been adapted in this paper to channel part of the negative energy invested by a human subject during walking, into electricity. Ultimately, this has been proven to reduce the metabolic effort of the subject during walking.

In contrary to vehicle braking, where the braking action is triggered by the user (by pressing the brake pedal), a biomechanical harvester must be capable of detecting the regions of negative work and applying the proper torque on the system, such that the energy is extracted and, at the same time, without interference to the natural motion. To this end, an adaptive algorithm that learns the walking pattern and estimates the harvesting profile has been developed.

The braking-harvesting action is facilitated in this paper by the torque applied on the knee joint. This is realized by a current-controlled boost converter that acts as a programmable load to a generator. In this context, a current sourcing behavior is essential for proper operation, since the torque of a synchronous machine is directly linked to its terminals' current.

To generalize the harvester solution onto any subject, walking profile, or duration, an optimal energy harvesting procedure has been developed. Based on a biofeedback from the user, the controller continuously optimizes the negative work detection procedure and the harvesting profile, such that the per-period COH is minimized. The results of the experiment upon a test subject demonstrate the feasibility to optimize the level of harvesting and find the minimum COH. Results further show that the metabolic energy can be reduced by the harvesting operation. This is also in agreement with recent publication that tested several different levels of external resistors to find the best COH [8].

This paper focused on the metabolic cost for generating the energy, yet it is obvious that for such a device to be successful, the mass of the device should be considered too. In [28], an approach is presented to determine what kind of portable power source should be considered (i.e., harvester or battery) based on the effort required by the user in each solution. That is, when both solutions provide the same amount of energy, the user would prefer a solution that requires less effort (metabolic cost). The effort for using the energy harvester is calculated as the summation of efforts for both carrying the device and the cost of generating the energy, whereas in the case of batteries, the metabolic cost for carrying a battery mass.

The findings in [28] show that a device with low mass (few hundred grams) with low COH (less than 1) could provide a good alternative to carrying batteries even if they produce low electrical energy ( $\sim 4$  W). A future aim in this paper is to improve the weight/power specifications of the harvester which currently stand at 1 kg/15 W. This will be carried out by reducing the weight of the brace.

The converter configuration, the control, and the tracking algorithm establish an infrastructure for future advanced research of braking torque shapes on the optimal amount of harvested energy and its effect on human subjects. Although demonstrated on a knee-joint harvesting device with metabolic rate as the human state parameter, the proposed approach can be applied to other joints and different human state parameters with some adjustments.

## REFERENCES

- [1] J. M. Donelan, Q. Li, V. Naing, J. A. Hoffer, D. J. Weber, and A. D. Kuo, "Biomechanical energy harvesting: Generating electricity during walking with minimal user effort," *Science*, vol. 319, no. 5864, pp. 807–810, Feb. 2008.
- [2] P. Niu, P. Chapman, R. Riemer, and X. Zhang, "Evaluation of motions and actuation methods for biomechanical energy harvesting," in *Proc. IEEE 35th Annu. Power Electron. Specialists Conf. (PESC)*, vol. 3, Jun. 2004, pp. 2100–2106.
- [3] R. Riemer and A. Shapiro, "Biomechanical energy harvesting from human motion: Theory, state of the art, design guidelines, and future directions," *J. NeuroEng. Rehabil.*, vol. 8, no. 1, p. 22, Dec. 2011.
- [4] J. A. Paradiso and T. Starner, "Energy scavenging for mobile and wireless electronics," *IEEE Pervasive Comput.*, vol. 4, no. 1, pp. 18–27, Jan./Mar. 2005.
- [5] R. E. Pelrine and R. D. Kornbluh, "Electroactive polymer devices," U.S. Patent 6545384, Apr. 8, 2003.
- [6] J. Y. Hayashida, "Unobtrusive integration of magnetic generator systems into common footwear," Ph.D. dissertation, Dept. Mech. Eng., Massachusetts Inst. Technol., Cambridge, MA, USA, 2000.
- [7] J. Granstrom, J. Feenstra, H. A. Sodano, and K. Farinholt, "Energy harvesting from a backpack instrumented with piezoelectric shoulder straps," *Smart Mater Struct.*, vol. 16, no. 5, pp. 1810–1820, Sep. 2007.
- [8] M. Shepetycky and Q. Li, "Generating electricity during walking with a lower limb-driven energy harvester: Targeting a minimum user effort," *PLoS ONE*, vol. 10, no. 6, pp. e0127635–1–e0127635-16, 2015.
- [9] D. A. Winter, "Energy generation and absorption at the ankle and knee during fast, natural, and slow cadences," *Clin. Orthopaedics*, vol. 175, pp. 147–154, May 1983.
- [10] D. A. Winter, *Biomechanics and Motor Control of Human Movement*, 3rd ed. Hoboken, NJ, USA: Wiley, 2005.
- [11] J. M. Donelan, R. Kram, and A. D. Kuo, "Simultaneous positive and negative external mechanical work in human walking," *J. Biomech.*, vol. 35, no. 1, pp. 117–124, Jan. 2002.
- [12] A. D. Kuo, "Harvesting energy by improving the economy of human walking," *Science*, vol. 309, no. 5741, pp. 1686–1687, Sep. 2005.
- [13] L. C. Rome, L. Flynn, E. M. Goldman, and T. D. Yoo, "Generating electricity while walking with loads," *Science*, vol. 309, no. 5741, pp. 1725–1728, Sep. 2005.
- [14] G. Wang, C. Luo, H. Hofmann, and L. Rome, "Power electronic circuitry for energy harvesting backpack," in *Proc. IEEE Energy Convers. Congr. Expo.*, Sep. 2009, pp. 3544–3549.
- [15] P. Niu, P. Chapman, L. DiBerardino, and E. Hsiao-Wecksler, "Design and optimization of a biomechanical energy harvesting device," in *Proc. IEEE Power Electron. Specialists Conf.*, Jun. 2008, pp. 4062–4069.
- [16] Q. Li, V. Naing, and J. M. Donelan, "Development of a biomechanical energy harvester," *J. NeuroEng. Rehabil.*, vol. 6, p. 22, Jun. 2009.
- [17] Q. Li, V. Naing, J. A. Hoffer, D. J. Weber, A. D. Kuo, and J. M. Donelan, "Biomechanical energy harvesting: Apparatus and method," in *Proc. IEEE Int. Conf. Robot. Autom.*, Pasadena, CA, USA, May 2008, pp. 3672–3677.
- [18] F. Yildiz, "Low power ambient energy harvesting, conversion, and storage circuits," in *Proc. 6th Int. Conf. Inf. Technol., New Generat.*, Apr. 2009, pp. 35–40.

- [19] R. Riemer, A. Shapiro, and S. Azar, "Optimal gear and generator selection for a knee biomechanical energy harvester," in *Proc. 1st Int. Conf. Appl. Bionics Biomech.*, Venice, Italy, 2010, pp. 14–16.
- [20] S. Mizrachi and R. Riemer, "Biomechanical energy harvesting: Control and evaluation of device efficiency," in *Proc. ICR*, Tel Aviv, Israel, 2013.
- [21] Z. Rubinshtein, M. M. Peretz, and R. Riemer, "Biomechanical energy harvesting system with optimal cost-of-harvesting tracking algorithm," in *Proc. IEEE Appl. Power Electron. Conf. (APEC)*, Mar. 2014, pp. 3105–3109.
- [22] Z. Rubinshtein, R. Riemer, and S. Ben-Yaakov, "Modeling and analysis of brushless generator based biomechanical energy harvesting system," in *Proc. IEEE Energy Convers. Congr. Expo. (ECCE)*, Sep. 2012, pp. 2784–2789.
- [23] J. F. Gieras and M. Wing, *Permanent Magnet Motor Technology*, 2nd ed. New York, NY, USA: Marcel Dekker, 2002.
- [24] T. Eswam and P. L. Chapman, "Comparison of photovoltaic array maximum power point tracking techniques," *IEEE Trans. Energy Convers.*, vol. 22, no. 2, pp. 439–449, Jun. 2007.
- [25] Maxon Motor Co., Sachseln, Switzerland. (2012). *Maxon EC 45 Flat 339285 Datasheet*. [Online]. Available: <http://www.maxonmotor.com>
- [26] Microchip Technology Inc., Chandler, AZ, USA. (2014). *PIC24FJ64GA104 Family Data Sheet*. [Online]. Available: <http://www.microchip.com>
- [27] J. M. Brockway, "Derivation of formulae used to calculate energy expenditure in man," *Human Nutrition. Clin. Nutrition*, vol. 41, no. 6, pp. 463–471, 1987.
- [28] E. Schertzer and R. Riemer, "Harvesting biomechanical energy or carrying batteries? An evaluation method based on a comparison of metabolic power," *J. NeuroEng. Rehabil.*, vol. 12, no. 30, pp. 1–12, Mar. 2015.



**Moran Gad** received the B.Sc. degree in mechanical engineering from the Ben-Gurion University of the Negev, Beersheba, Israel, in 2012, where he is currently working toward the M.Sc. degree.

He has been a part of the biomechanical energy harvesting team since 2010, and is dealing with the harvester mechanics, mathematical models, and the optimization of the harvester system. He is the Head of Research and Development with Motionize Inc., Tel Aviv, Israel.



**Raziel Riemer** received the B.Sc. degree in mechanical engineering and the M.Sc. degree in industrial engineering with concentration in robotics from the Ben-Gurion University of the Negev, Beersheba, Israel, in 1993 and 1996, respectively, and the Ph.D. degree in mechanical engineering from the University of Illinois at Urbana-Champaign, Champaign, IL, USA, in 2006.

He continued his post-doctoral studies with the Ben-Gurion University of the Negev. He is currently a Faculty Member with the Department of Industrial and Management Engineering, Ben-Gurion University of the Negev. He was an Engineer with the industry for six years, prior to joining academia. He is the Director of the Biomechanics and Robotics Laboratory with the Department of Industrial and Management Engineering, Ben-Gurion University of the Negev. His current research interests include analysis, modeling, and simulation of human movement, and robotics. He integrates knowledge from biomechanics and robotics. This research has implications for ergonomics, robotics, and biomechanical energy harvesting.



**Alon Cervera** (S'12) was born in London, U.K., in 1985. He received the B.Sc. and M.Sc. degrees in electrical and computer engineering from the Ben-Gurion University of the Negev, Beersheba, Israel, in 2011 and 2013, respectively, where he is currently working toward the Ph.D. degree in electrical and computer engineering.

His current research interests include switched-capacitor converters, voltage regulation techniques, envelope-tracking renewable energy systems, and digital control.



**Ze'ev Rubinshtein** received the B.Sc. and M.Sc. degrees in electronic and computer engineering from the Ben-Gurion University of the Negev, Beersheba, Israel, in 2010 and 2013, respectively.

He is currently a Research and Development Engineer in Power Electronics with the Ben-Gurion University of the Negev. His current research interests include renewable energy systems, smart control for switch-mode power supplies (SMPS), and magnetic design.



**Mor Mordechai Peretz** (S'05–M'12) was born in Beersheba, Israel, in 1979. He received the B.Tech. degree in electrical engineering from the Negev Academic College of Engineering, Beersheba, in 2003, and the M.Sc. and Ph.D. degrees in electrical and computer engineering from the Ben-Gurion University of the Negev, Beersheba, in 2005 and 2010, respectively.

He was a Post-Doctoral Fellow with the Laboratory for Power Management and Integrated SMPS, University of Toronto, Toronto, ON, Canada, from 2010 to 2012. In 2012, he joined the Department of Electrical and Computer Engineering, Ben-Gurion University of the Negev, where he is currently the Director of the Center for Power Electronics and Mixed-Signal IC. His current research interests include digital and smart control methods for efficient energy processing, SMPS miniaturization, mixed-signal IC design of SMPS, modeling and computer aided design, applications of nonlinear magnetics, and renewable energy systems.

Dr. Peretz serves as an Associate Editor of the IEEE TRANSACTIONS ON POWER ELECTRONICS and the IEEE JOURNAL OF EMERGING AND SELECTED TOPICS IN POWER ELECTRONICS.